

Drive control algorithm for an independent 8 in-wheel motor drive vehicle[†]

Wongun Kim¹, Kyongsu Yi^{2,*} and Jongseok Lee³

¹Program in Automotive Engineering, Seoul National University, Seoul, 151-742, Korea

²School of Mechanical and Aerospace Engineer, Seoul National University, Seoul, 151-742, Korea

³Samsung Techwin, 69-2, Sinchon-Dong, Changwon, Kyungnam-do, Korea

(Manuscript Received June 22, 2010; Revised March 28, 2011; Accepted March 30, 2011)

Abstract

This paper describes a drive control algorithm based on optimal coordination of drive torque for an independent 8 in-wheel motor drive vehicle. The drive controller improves lateral stability and maneuverability. The drive controller consists of upper level controller and lower level controller. The upper level controller determines front, middle steering angle, additional net yaw moment and longitudinal net force according to the reference velocity and steering commands. The lower level controller coordinates additional tractive and braking forces to guarantee desired longitudinal net force and yaw moment. This controller is based on optimal control theory and takes into consideration the friction circle related to the vertical tire force and friction coefficient acting on the road and tire. Distributed tractive and braking forces are determined as proportional to the size of the friction circle according to the changes at driving conditions. The response of the 8 in-wheel drive vehicle implemented with this drive controller has been evaluated via computer simulations conducted using Matlab/Simulink dynamic model. Computer simulations of an open-loop J-turn maneuver and a closed-loop driver model subjected to double lane change have been conducted to demonstrate improved performance and stability of the proposed drive controller.

Keywords: Drive controller; Sliding control; Optimal distribution; Yaw moment control; Friction circle estimation; In-wheel drive system

1. Introduction

An independent eight wheel drive / four wheel steering vehicle (8WD/4WS) mechanism has been adopted for use in a special purposed, military armored vehicle to enhance steering performance and drive capability on off-road and on-road. The 8WD/4WS vehicle is believed to have better performance than a conventional vehicle in terms of obstacle navigation, off-road and on-road maneuvering. Six or eight wheeled combat vehicles have been used to conduct battles on city streets. Therefore, many researches of wheeled combat vehicle have been conducted.

Various methods have been studied and actively developed to improve lateral stability of a four-wheeled vehicle [1-4]. Jackson and Crolla (2002) proposed yaw rate control method using direct yaw moment control (DYC) [5] to improve the stability of their six-wheeled vehicle during cornering. Chen et al. controlled the middle and rear steering angle in order to guarantee vehicle stability and improve maneuverability using the LQR technique with integral control [6]. An et al. have controlled the front, middle and rear wheel steering angle and

vehicle velocity [7, 8].

In previous research, vehicles were equipped with engine and transmission. Only brake torque was used to generate the desired yaw moment and wheel output torques could not be determined independently. Therefore, previous researchers designed a controller without the consideration of changes in each wheel load conditions. Performance of the stability controller may be limited. However, the proposed 8WD/4WS vehicle is classified as an electric heavy vehicle and equipped with an x-by-wire independent drive, steering and braking system. An electric heavy vehicle has many advantages such as high efficiency, maneuverability, stability and stealth mode driving. It is important to develop the drive controller considering wheel load conditions for an 8WD/4WS vehicle in order to guarantee stability and improve maneuverability. In this paper, a drive controller for lateral stability and maneuvering improvement has been designed. Numerical simulation has been conducted to verify performance of the proposed drive controller.

2. Vehicle dynamic model

The 8WD/4WS vehicle is modeled as an object with 26 degrees-of-freedom (DOF). The full vehicle model consists of 6 DOF translational (Eq. (1)) and rotational (Eq. (2)) dynamic models of the sprung mass, 8 suspension models (Eq. (3)), 8

[†] This paper was recommended for publication in revised form by Editor Long Wang

*Corresponding author. Tel.: +82 2 880 1941, Fax.: +82 2 880 1942

E-mail address: kyi@snu.ac.kr

© KSME & Springer 2011

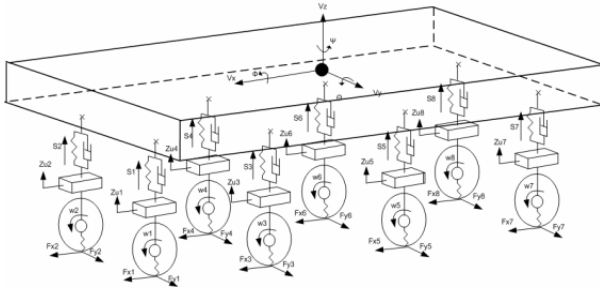


Fig. 1. Vehicle dynamic model.

wheel dynamics (Eq. (4)) and 4 steering dynamics (Eq. (5)).

$$\sum F = m_s a_G \quad \Sigma F_x = m_s(a_x + v_y w_z - v_z w_y), \quad \Sigma F_y = m_s(a_y + v_x w_z - v_z w_x), \quad \Sigma F_z = m_s(a_z + v_y w_x - v_x w_y), \quad (1)$$

$$\sum M = \dot{H}_g \quad \Sigma M_x = I_x a_x + (I_z - I_y) w_y w_z, \quad \Sigma M_y = I_y a_y + (I_x - I_z) w_z w_x, \quad \Sigma M_z = I_z a_z + (I_y - I_x) w_x w_y, \quad (2)$$

$$\ddot{z}_{ui} = \frac{1}{m_{ui}} \left\{ -K_{ti}(z_{ui} - z_{ri}) + \frac{K_{ri}}{t_i} \phi - F_{si} \right\}, \quad (3)$$

$$J_w \cdot \frac{d\omega_i}{dt} = T_i - r_i \cdot F_{i_tirex}, \quad (4)$$

$$I_{Hi} \frac{d^2 \delta_i}{dt^2} + K_C(\delta_i - \theta_{Ci}) = T_{Hi}. \quad (5)$$

Longitudinal and lateral tire models are designed using the Pacejka tire modeling method. Power of motor model is 120 kW and maximum torque is 12 kNm. The full vehicle dynamic model makes it possible to analyze the 8WD/4WS vehicle's maneuverability and to study the control method for the drive controller. The vehicle dynamic model was developed using Matlab/Simulink in order to conduct numerical simulation studies. An 8WD/4WS vehicle equipped with 8 in-wheel-motors is able to operate in differential traction and braking drive modes. Fig. 2 shows the Pacejka tire model and the performance curve of in-wheel motors.

Table 1 shows parameters of an 8WD/4WS vehicle which is classified as a heavy combat vehicle for military purpose.

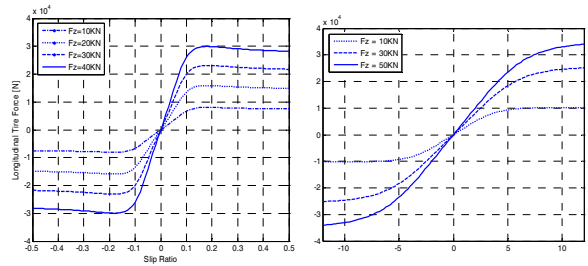
3. Controller design

The proposed x-by-wire system in an 8WD/4WS vehicle is able to control the traction and handling independently. Fig. 3 shows the drive control strategy of the drive controller. Since it is difficult to determine the wheel torque command directly, the drive control algorithm was designed for the 8WD/4WS vehicle with three parts as follows: upper level, lower level and wheel slip controller.

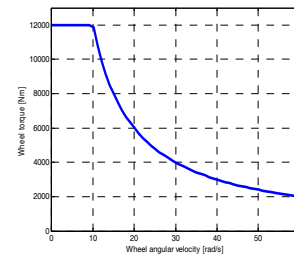
Maneuverability and stability performance of the drive controller are superior to those of other vehicles equipped with engine, transmission and differential gear. Fig. 4 shows the

Table 1. Specification of an 8WD/4WS vehicle.

Parameter	Value	Parameter	Value
Sprung Mass(ms)	18650 [kg]	Moment inertia (Izz)	97303 [kgm ²]
Unsprung mass(mu)	362.0 [kg]	Track Width(t)	2.264 [m]
Wheel base (L)	4.6 [m]	Tire radius (ri)	0.56 [m]
Wheel moment inertia (J _w)	14 [kgm ²]	Steering column inertia (I _H)	0.034 [kgm ²]
Suspension spring stiffness (K _{ti})	80000 [N/m]	Rollbar stiffness (K _{ri})	326010 [Nm/rad]
Tire stiffness (K _r)	560000 [N/m]	Steering column stiffness (K _C)	50000 [Nm/rad]



(a) Longitudinal tire model (b) Lateral tire model



(c) In-wheel motor model

Fig. 2. Tire and motor of a vehicle dynamic model.

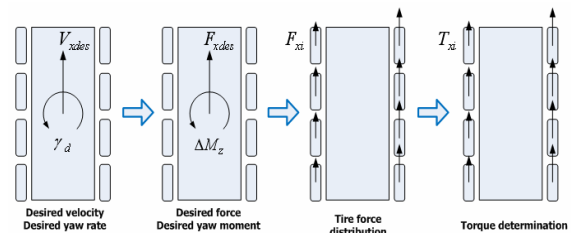


Fig. 3. The control strategy of the drive controller.

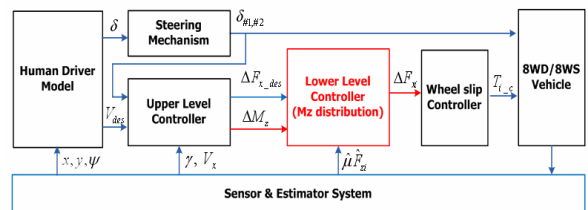


Fig. 4. The drive control algorithm block diagram.

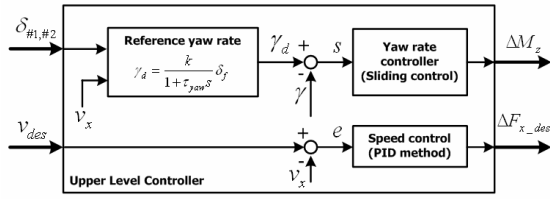


Fig. 5. The upper level control block diagram.

drive control block diagram. The drive controller consists of upper level and lower level controller.

3.1 Upper level controller

The upper level controller takes the driver’s steering input and reference velocity as inputs. It determines the desired longitudinal net tire force and yaw moment. Fig. 5 shows the upper level controller.

The upper level controller consists of determination of first/second axle wheel angle, calculation of reference yaw rate, yaw rate controller and speed controller. The 8WD/4WS vehicle is difficult to generate efficient turning motion using only steering wheel angle on the first axle. For efficient turning drive, second axle steering angle is defined as a function of the first axle steering angle. And it needs to satisfy the Ackerman steering relation. The second axle steering angle is written as a wheel base and length from the center of gravity to the first/second axle.

$$\delta_{\#2} = \delta_{\#1} - (l_{\#1} - l_{\#2}) / \rho = \delta_{\#1} (L - l_{\#1} + l_{\#2} / L). \quad (6)$$

It is necessary to consider slip effects on high speed condition. Therefore, the desired yaw rate is defined as a four wheel bicycle model for the drive controller of the 8WD/4WS vehicle. The dynamic model is defined as first order differential equation as follows:

$$\dot{x} = A_{opt} \cdot x + B_{opt} \cdot u \quad (7)$$

$$A_{opt} = \begin{bmatrix} \frac{-2(C_{\#1} + C_{\#2} + C_{\#3} + C_{\#4})}{mv_x} & \frac{-2(l_{\#1}C_{\#1} + l_{\#2}C_{\#2} - l_{\#3}C_{\#3} - l_{\#4}C_{\#4})}{mv_x^2} - 1 \\ \frac{-2(l_{\#1}C_{\#1} + l_{\#2}C_{\#2} - l_{\#3}C_{\#3} - l_{\#4}C_{\#4})}{I_z} & \frac{-2(l_{\#1}^2C_{\#1} + l_{\#2}^2C_{\#2} + l_{\#3}^2C_{\#3} + l_{\#4}^2C_{\#4})}{I_z v_x} \end{bmatrix}$$

$$B_{opt} = \begin{bmatrix} \frac{2C_{\#1}}{mv_x} & \frac{2C_{\#2}}{mv_x} \\ \frac{2l_{\#1}C_{\#1}}{I_z} & \frac{2l_{\#2}C_{\#2}}{I_z} \end{bmatrix} = \begin{bmatrix} b_{11} & b_{12} \\ b_{21} & b_{22} \end{bmatrix}, \quad x = \begin{bmatrix} \beta \\ \gamma \end{bmatrix}, \quad u = \begin{bmatrix} \delta_{\#1} \\ \delta_{\#2} \end{bmatrix}.$$

A steady state bicycle model is useful to determine the steady state desired yaw rate from steering angle of the first and second axes. The steady state yaw rate is defined as follows:

$$\gamma_{ss} = \frac{(a_{21}b_{11} - a_{11}b_{21})\delta_{\#1} + (a_{21}b_{12} - a_{11}b_{22})\delta_{\#2}}{(a_{11}a_{22} - a_{12}a_{21})}. \quad (8)$$

The desired yaw rate is determined by steady state yaw rate and first order transfer function as follows:

$$\gamma_d = \frac{1}{1 + \tau_{yaw}s} \gamma_{ss}. \quad (9)$$

The desired yaw rate is reasonably constrained by the physical limit of tire-road friction as follows:

$$|\gamma_d| \leq \mu g / v_x. \quad (10)$$

To track the proposed single target yaw rate, a yaw rate controller is designed by 2 DOF bicycle model. Proposed yaw rate controller based on sliding mode control theory calculates required yaw moment to stabilize the vehicle. The yaw rate dynamics is considered as the first order single input dynamic system as follows:

$$I_z \dot{\gamma} = 2l_{\#1}F_{y\#1} + 2l_{\#2}F_{y\#2} - 2l_{\#3}F_{y\#3} - 2l_{\#4}F_{y\#4} + \Delta M_z. \quad (11)$$

The sliding surface is defined by yaw rate error as follows:

$$s = \gamma - \gamma_d. \quad (12)$$

The control objective is to make the sliding surface converge to zero. It can be achieved by choosing the control law satisfying the sliding condition states as follows:

$$\frac{1}{2} \frac{d}{dt} s^2 \leq -\eta |s|. \quad (\eta > 0). \quad (13)$$

The sliding control law is defined as a required yaw moment as follows:

$$\Delta M_z = -2l_{\#1}F_{y\#1} - 2l_{\#2}F_{y\#2} + 2l_{\#3}F_{y\#3} + 2l_{\#4}F_{y\#4} + I_z \cdot \dot{\gamma}_d - I_z \cdot \eta \cdot s \operatorname{sat}\left(\frac{s}{\Phi}\right). \quad (14)$$

3.2 Lower level controller (optimal distribution)

The lower level controller is designed to distribute additional tractive/braking forces in order to generate the desired longitudinal net force and yaw moment. Control objectives of the lower level controller are to minimize control input and to determine distributed tire forces in proportion to the size of a friction circle which changes according to the drive conditions. A friction circle means that maximum tire force can be generated by on each wheel. The performance index can be defined as a combination of control inputs, friction circle and weighting factors. Proposed performance index has been selected as follows [9]:

$$J = \frac{c_{x1}\Delta F_{x1}^2}{(\mu_1 F_{z1})^2} + \frac{c_{x2}\Delta F_{x2}^2}{(\mu_2 F_{z2})^2} + \frac{c_{x3}\Delta F_{x3}^2}{(\mu_3 F_{z3})^2} + \frac{c_{x4}\Delta F_{x4}^2}{(\mu_4 F_{z4})^2} + \frac{c_{x5}\Delta F_{x5}^2}{(\mu_5 F_{z5})^2} + \frac{c_{x6}\Delta F_{x6}^2}{(\mu_6 F_{z6})^2} + \frac{c_{x7}\Delta F_{x7}^2}{(\mu_7 F_{z7})^2} + \frac{c_{x8}\Delta F_{x8}^2}{(\mu_8 F_{z8})^2} \tag{15}$$

Weighting factors ($c_{x1}, c_{x2}, \dots, c_{x8}$) contained in the performance index can improve performance of the drive controller according to various driving conditions. In this paper, weighting factors are set to one. Control inputs should be satisfied with constraints related to desired net force and yaw moment. Constraints are written as follows:

$$\Delta F_{x_des} = \Delta F_{x1} + \Delta F_{x2} + \Delta F_{x3} + \Delta F_{x4} + \Delta F_{x5} + \Delta F_{x6} + \Delta F_{x7} + \Delta F_{x8} \tag{16}$$

$$\Delta M_z = \frac{t}{2} \{-\Delta F_{x1} + \Delta F_{x2} - \Delta F_{x3} + \Delta F_{x4} - \Delta F_{x5} + \Delta F_{x6} - \Delta F_{x7} + \Delta F_{x8}\} \tag{17}$$

The number of independent variables that the problem contains has been changed from eight to six using two constraints as follows:

$$\Delta F_{x7} = -\frac{\Delta M_z}{t} - \Delta F_{x1} - \Delta F_{x3} - \Delta F_{x5} + \frac{\Delta F_{x_des}}{2} \tag{18}$$

$$\Delta F_{x8} = \frac{\Delta M_z}{t} - \Delta F_{x4} - \Delta F_{x6} - \Delta F_{x2} + \frac{\Delta F_{x_des}}{2} \tag{19}$$

Six independent variables that were previously defined can be solved by optimal control method. It is the necessary condition that minimizes the performance index. Independent variable x is defined and should be satisfied with the reformulated equation as follows:

$$Ax = B, \quad x = [\Delta F_{x1} \quad \Delta F_{x2} \quad \Delta F_{x3} \quad \Delta F_{x4} \quad \Delta F_{x5} \quad \Delta F_{x6}]^T \tag{20}$$

$$A = \begin{bmatrix} 2\left(\frac{c_{x1}}{(\mu_1 F_{z1})^2} + \frac{c_{x7}}{(\mu_7 F_{z7})^2}\right) & 0 & 2\cdot\frac{c_{x7}}{(\mu_7 F_{z7})^2} \\ 0 & 2\left(\frac{c_{x2}}{(\mu_2 F_{z2})^2} + \frac{c_{x8}}{(\mu_8 F_{z8})^2}\right) & 0 \\ 2\cdot\frac{c_{x7}}{(\mu_7 F_{z7})^2} & 0 & 2\left(\frac{c_{x3}}{(\mu_3 F_{z3})^2} + \frac{c_{x7}}{(\mu_7 F_{z7})^2}\right) \\ 0 & 2\cdot\frac{c_{x8}}{(\mu_8 F_{z8})^2} & 0 \\ 2\cdot\frac{c_{x7}}{(\mu_7 F_{z7})^2} & 0 & 2\cdot\frac{c_{x7}}{(\mu_7 F_{z7})^2} \\ 0 & 2\cdot\frac{c_{x8}}{(\mu_8 F_{z8})^2} & 0 \\ 0 & 2\cdot\frac{c_{x7}}{(\mu_7 F_{z7})^2} & 0 \\ 2\cdot\frac{c_{x8}}{(\mu_8 F_{z8})^2} & 0 & 2\cdot\frac{c_{x8}}{(\mu_8 F_{z8})^2} \\ 0 & 2\cdot\frac{c_{x7}}{(\mu_7 F_{z7})^2} & 0 \\ 2\left(\frac{c_{x4}}{(\mu_4 F_{z4})^2} + \frac{c_{x8}}{(\mu_8 F_{z8})^2}\right) & 0 & 2\cdot\frac{c_{x8}}{(\mu_8 F_{z8})^2} \\ 0 & 2\left(\frac{c_{x5}}{(\mu_5 F_{z5})^2} + \frac{c_{x7}}{(\mu_7 F_{z7})^2}\right) & 0 \\ 2\cdot\frac{c_{x8}}{(\mu_8 F_{z8})^2} & 0 & 2\left(\frac{c_{x6}}{(\mu_6 F_{z6})^2} + \frac{c_{x8}}{(\mu_8 F_{z8})^2}\right) \end{bmatrix}$$

$$B = \begin{bmatrix} -2\cdot\frac{c_{x7}}{(\mu_7 F_{z7})^2}\cdot\frac{\Delta M_z}{t} + \frac{c_{x7}}{(\mu_7 F_{z7})^2}\cdot\Delta F_{x_des} \\ +2\cdot\frac{c_{x8}}{(\mu_8 F_{z8})^2}\cdot\frac{\Delta M_z}{t} + \frac{c_{x8}}{(\mu_8 F_{z8})^2}\cdot\Delta F_{x_des} \\ -2\cdot\frac{c_{x7}}{(\mu_7 F_{z7})^2}\cdot\frac{\Delta M_z}{t} + \frac{c_{x7}}{(\mu_7 F_{z7})^2}\cdot\Delta F_{x_des} \\ +2\cdot\frac{c_{x8}}{(\mu_8 F_{z8})^2}\cdot\frac{\Delta M_z}{t} + \frac{c_{x8}}{(\mu_8 F_{z8})^2}\cdot\Delta F_{x_des} \\ -2\cdot\frac{c_{x7}}{(\mu_7 F_{z7})^2}\cdot\frac{\Delta M_z}{t} + \frac{c_{x7}}{(\mu_7 F_{z7})^2}\cdot\Delta F_{x_des} \\ +2\cdot\frac{c_{x8}}{(\mu_8 F_{z8})^2}\cdot\frac{\Delta M_z}{t} + \frac{c_{x8}}{(\mu_8 F_{z8})^2}\cdot\Delta F_{x_des} \end{bmatrix}$$

Matrices of A and B are expressed by friction circle, tread, wheel base, desired longitudinal net force and yaw moment. This linear system can be solved at each time step to find the distribution of optimal tire forces.

3.3 Wheel slip control

The wheel slip controller is designed to keep the slip ratio of each wheel below the maximum slip ratio as well as to track the desired longitudinal tire force. Fig. 6 shows the strategy of the wheel slip control algorithm. In the case of small slip ratio below the maximum slip ratio, wheel torque command, which is determined by the lower level controller, is passed directly to in-wheel motor driver. However, in the case of high slip ratio above the maximum slip ratio, the wheel slip controller calculates new control input to regulate exceeding the maximum slip ratio using wheel speed control method.

On wheel speed control mode, the wheel slip controller defines desired wheel speed using absolute longitudinal velocity and maximum slip ratio (λ_{max}). In this paper, the maximum

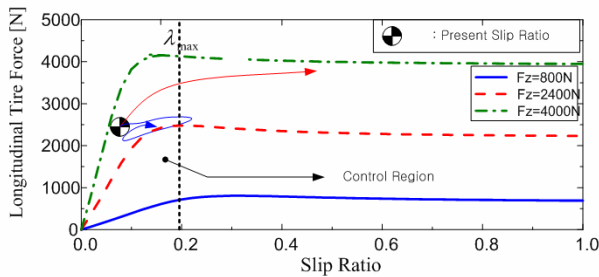


Fig. 6. Strategy of the wheel slip controller.

wheel slip ratio is set to 0.2 in order to guarantee lateral tire forces. The desired wheel speed is determined differently depending on driving conditions such as traction and braking as follows:

$$\omega_{id} = \begin{cases} \frac{v_i}{r_i(1-\lambda_{max})} & \text{if } (\lambda > \lambda_{max}) \text{ Driving} \\ \frac{v_i}{r_i}(1-\lambda_{max}) & \text{if } (\lambda < -\lambda_{max}) \text{ Braking} \end{cases} \quad (21)$$

The wheel slip controller is based on sliding control method [10]. The sliding surface is defined by wheel angular velocity error as follows:

$$s = \omega - \omega_{id} \quad (22)$$

The derivative of the sliding surface should be satisfied to determine control input which converges to zero.

$$\dot{s} = \dot{\omega} - \dot{\omega}_{des} = \frac{1}{J} \{ T - r \cdot \hat{F}_x \} - \dot{\omega}_{des} \leq -\eta \cdot \text{sgn}(s) \quad (23)$$

In the case of the wheel slip ratio exceeding the maximum slip ratio, wheel torque commands are determined based on sliding control law. Except for the above case, wheel torque commands are determined by distributed longitudinal tire force and wheel radius.

$$\begin{cases} T = r_i \cdot \Delta F_{xi} & |\lambda| < \lambda_{max} \\ T = J \dot{\omega}_{des} + r \cdot \hat{F}_x - J \eta \cdot \text{sgn}(s) & \text{Otherwise} \end{cases} \quad (24)$$

It is necessary that the estimated longitudinal tire force needs to be calculated to determine control inputs. The estimation of longitudinal tire force will be described in detail in the next section.

4. Friction circle estimation [11]

For the implementation of the drive controller, it is important to know the vertical tire force and friction coefficient. However, measurement of this information is difficult or expensive. Therefore, friction circle estimation needs to be conducted to coordinate optimal distribution of tire forces on the drive controller. Friction circle means the maximum tire force which can be generated on each wheel, that is, the friction circle represents multiplication of the vertical tire force and friction coefficient. Estimating the friction circle is more convenient than estimating the vertical tire force and the friction coefficient separately on various driving conditions. The estimator consists of longitudinal tire force, slip ratio and friction circle estimation as shown in Fig. 7. The required sensor signals are the longitudinal vehicle velocity, wheel speed and wheel torque. The longitudinal vehicle velocity can be measured easily from integrated GPS/INS system.

5. Human driver model for closed-loop simulation

The human driver model [12] is designed to evaluate per-

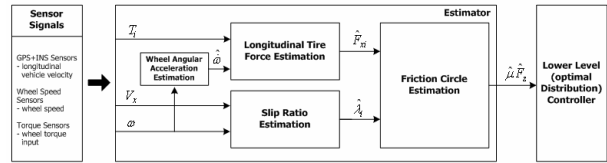


Fig. 7. Configuration of Friction circle estimation.

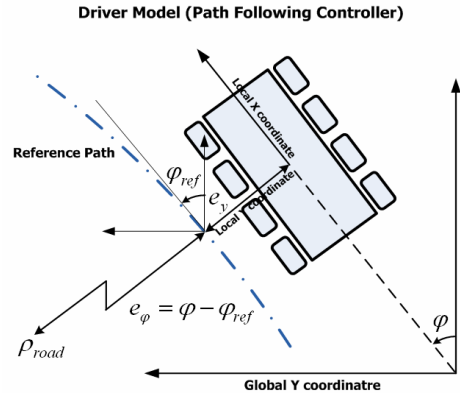


Fig. 8. Path tracking control system modeling.

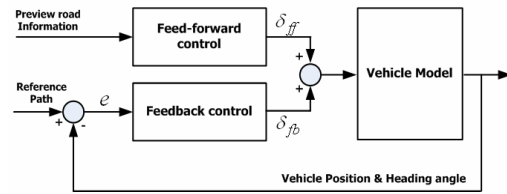


Fig. 9. Path tracking control system modeling.

formance of the drive controller. The model based on path tracking control algorithm determines a driver's steering input instead of real driver. First, path tracking control system modeling should be performed. Fig. 8 shows path tracking control modeling. States of control system are defined as lateral position error and angle error between vehicle and road.

The state equation of error dynamics can be obtained by lateral error, derivative of lateral error, road angle error and derivative of road angle error as follows:

$$\dot{e} = Ae + Bu + Fw = Ae + B\delta + F\dot{\varphi}_d \quad (25)$$

where $e = [y_r \quad \dot{y}_r \quad \varphi - \varphi_d \quad \dot{\varphi} - \dot{\varphi}_d]^T$

$$\frac{d}{dt} \begin{bmatrix} e_y \\ \dot{e}_y \\ e_\varphi \\ \dot{e}_\varphi \end{bmatrix} = \begin{bmatrix} 0 & 1 & 0 & 0 \\ 0 & \frac{-2(C_f + C_r)}{mv_x} & \frac{2(C_f + C_r)}{m} & \frac{-2(l_f C_f - l_r C_r)}{mv_x} \\ 0 & 0 & 0 & 1 \\ 0 & \frac{-2(l_f C_f - l_r C_r)}{I_z v_x} & \frac{2(l_f C_f - l_r C_r)}{I_z} & \frac{-2(l_f^2 C_f + l_r^2 C_r)}{I_z v_x} \end{bmatrix} \begin{bmatrix} e_y \\ \dot{e}_y \\ e_\varphi \\ \dot{e}_\varphi \end{bmatrix} + \begin{bmatrix} 0 \\ \frac{2C_f}{m} \\ 0 \\ \frac{2l_f C_f}{I_z} \end{bmatrix} \delta + \begin{bmatrix} 0 \\ \frac{-2(l_f C_f - l_r C_r)}{mv_x} - v_x \\ 0 \\ \frac{-2(l_f^2 C_f + l_r^2 C_r)}{I_z v_x} \end{bmatrix} \dot{\varphi}_d$$

The control strategy of the path tracking is to eliminate lateral error and yaw angle error through a combination of feedback and feed-forward control law as follows:

$$u = u_{fb} + u_{ff} = -K_{opt}e - B^{-1}Fw. \tag{26}$$

The feedback control law based on optimal control theory is computed using error dynamic states. Feed-forward control law is determined by using preview road information. Control input u is steering angle.

Error dynamic equation can be rewritten as follows:

$$\dot{e} = Ae + Bu + Fw = Ae + Bu_{fb}. \tag{27}$$

The feedback control gain (K_{opt}) is obtained by minimizing the performance index J defined as follows:

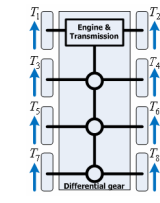
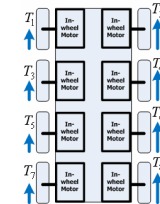
$$J = \lim_{t_f \rightarrow \infty} \frac{1}{2} E \left[\frac{1}{2} \int_0^{t_f} (e^T Q e + u_{fb}^T R u_{fb}) dt \right]. \tag{28}$$

Q and R are the weighting matrices for state deviations and input efforts, respectively.

6. Numerical simulation

The response of the 8WD/4WS vehicle implemented with the drive controller has been evaluated via computer simula-

Table 2. Two drive schemes of an 8WD/4WS vehicle.

Simulation Case	Description	Illustration
Case I	Even distribution, equipped with engine, transmission	
Case II	Optimal distribution, equipped with in-wheel motors	

tions. Open-loop and closed-loop simulations using a human driver model have been conducted to verify the improved performance of the proposed drive controller. Two drive schemes for an eight wheeled vehicle are described in Table 2. In case I, drive torques are evenly distributed on each wheel. In case II, the optimal drive torque distribution proposed in this study has been used.

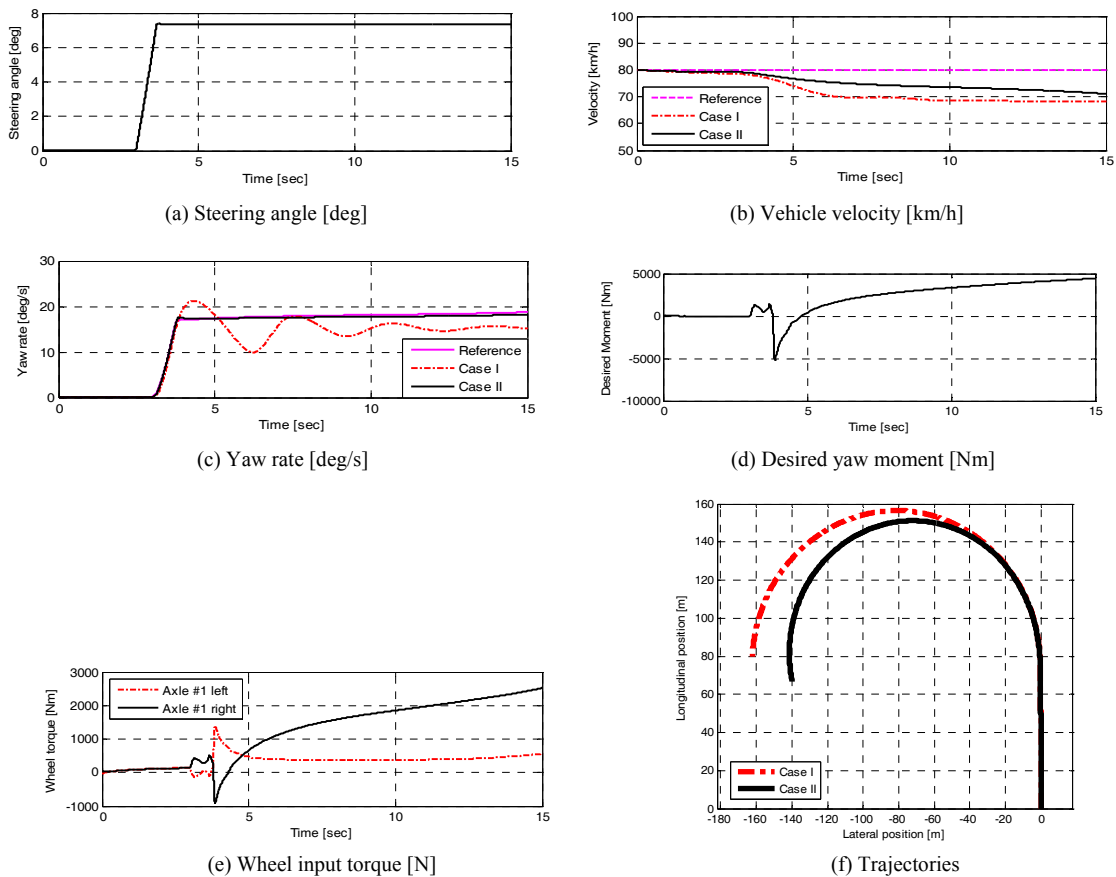


Fig. 10. Open-loop simulation results.

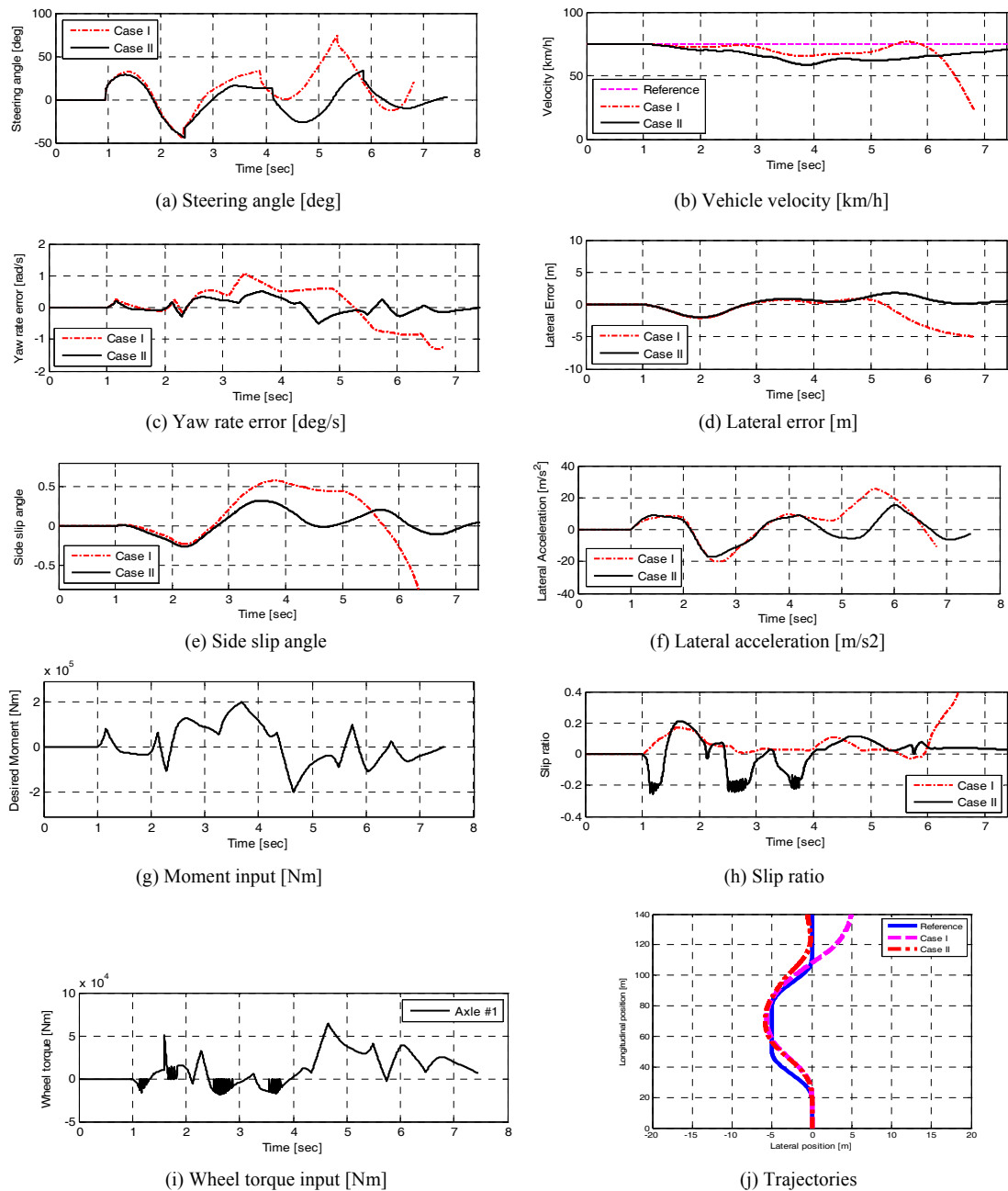


Fig. 11. Closed-loop simulation results.

6.1 Open-loop control simulation

An open-loop simulation has been conducted to verify the performance of the drive controller. Fig. 10 shows simulation results for J-turn maneuver on 0.6 low friction coefficients. Initial longitudinal vehicle velocity is set to 80 km/h and steering input is step steer as shown in Fig. 10(a). The proposed drive controller enhances performance of maneuverability with respect to longitudinal velocity and yaw rate of the vehicle. Fig. 10(b) shows vehicle velocity of the reference, case I and case II. Vehicle velocity of case II is larger than that of case I. This is because differential drive torques are generated

to satisfy the reference yaw rate and reference vehicle velocity. Yaw rate of the case II follows the reference yaw rate accurately as shown in Fig. 10(c). Desired yaw moment and wheel input torque are determined to guarantee low level of yaw rate error as shown in Fig. 10(d) and (e).

6.2 Closed-loop control simulation

In closed-loop control simulation, initial vehicle velocity is 80 km/h and friction coefficient is changed from 0.9 to 0.5 at right wheel (split- μ). Simulation results for double lane change are shown in Fig. 11(a) shows steering input which is

determined to path tracking control. Fig. 11(b) is longitudinal vehicle velocity of reference, case I and case II. The drive controller (case II) enhances performance over the case I with respect to the yaw rate error, lateral position error and side slip angle as shown in Fig. 11(c), (d) and (e). In Fig. 11(f), lateral stability of case II is guaranteed within smaller level of side slip angle and lateral acceleration than case I. Yaw moment input is determined to maintain vehicle stability. Slip ratio of the case I exceeds the maximum slip ratio. However, in case II, the drive controller keeps slip ratio to the maximum slip ratio as shown in Fig. 11(h).

7. Conclusions

A drive control algorithm for an 8WD/4WS vehicle to improve vehicle stability and maneuverability has been proposed. The drive controller is based on optimal distribution control and considering the friction circle related to vertical tire force and friction coefficient acting on the road and tire. The friction circle is estimated using vehicle state information which can be measured by sensors. The response of the 8WD/4WS vehicle with the drive controller has been evaluated via computer simulations using Matlab /Simulink dynamic model. Simulation results show that performance and stability of the proposed drive controller is better than that of simple drive controller (even distribution, Case I) with respect to the yaw rate, lateral position error, side slip angle and slip ratio. It has been shown that maneuverability of the 8WD /4WS vehicle can be significantly improved by the use of the proposed drive controller compared to a simple drive controller.

Acknowledgment

This work has been supported by the Samsung Techwin, the BK 21 Program, the SNU-IAMD, the Korea Research Foundation Grant funded by the Korean Government (MEST) (KRF-2009-200-D00003), National Research Foundation of Korea Grant funded by the Korean Government (2009-0083495) and the Agency to Defense Development.

Nomenclature

$C_{\#i}$: Cornering stiffness of i-th axle wheel [N]
$F_{y\#i}$: Lateral tire force of i-th axle wheel [N]
F_{zi}	: Vertical tire force of i-th wheel [N]
F_{si}	: Suspension Force of i-th wheel [N]
I_z	: Z_axis moment of inertia [kgm ²]
J_{ω}	: Moment of inertia of each wheel [kgm ²]
L	: Wheel base [m]
T_i	: Input tractive/brake torque command of i-th wheel [Nm]
T_{Hi}	: Input steering torque command of i-th wheel [Nm]
V_{des}	: Desired longitudinal vehicle velocity [km/h]
c_{xi}	: Weighting factors of i-th wheel
g	: Gravity acceleration [m/s ²]
$l_{\#i}$: Distance from C.G to i-th wheel axle [m]

r_i	: Tire radius of i-th wheel [m]
t	: Track width of the vehicle [m]
v_x	: Vehicle velocity [m/s]
x	: Vehicle position of x-axis [m]
y	: Vehicle position of y-axis [m]
z_{ui}	: Displacement of a unsprung mass [m]
z_{ri}	: Displacement of a road profile [m]
α_i	: Slip angle of i-th wheel [rad]
β	: Side slip angle
γ	: Yaw rate [rad/s]
γ_d	: Desired yaw rate [rad/s]
γ_{ss}	: Steady state yaw rate [rad/s]
$\delta_{\#i}$: Steering wheel angle of i-th axle [rad]
θ	: Pitch angle of the vehicle [rad]
θ_{Ci}	: Steering column angle of i-th wheel [rad]
λ_i	: Slip ratio of i-th wheel
μ	: Friction coefficient of the road
ρ	: Distance from C.G to turning center point [m]
ϕ	: Roll angle of the vehicle [rad]
ψ	: Yaw angle of the vehicle [rad]
τ_{yaw}	: Time delay constant of desired yaw rate calculation [s]
ω_i	: Wheel angular velocity of i-th wheel [rad/s]
ω_{id}	: Desired wheel angular velocity of i-th wheel [rad/s]
ΔM_z	: Requirement of yaw moment [Nm]
ΔF_{x_des}	: Additional longitudinal net tire force [N]
ΔF_{xi}	: Additional tractive/braking force of i-th wheel [N]

References

- [1] A. T. Zanten, R. Erhardt, K. Landesfeind and G. Pfaff, VDC Systems development a yaw moment control using braking forces, *JSME International Journal*, 42 (2) (1999) 301-308.
- [2] Y. Shibahata, K. Shimada and T. Tomari, The improvement of vehicle maneuverability by direct yaw moment control, *Proc. Int. Symp. Advanced Vehicle Control* (1992) 452-457.
- [3] T. Shino and M. Nagai, Yaw moment control of electric vehicle for improving handling and stability, *JSAE Review* 22 (2001) 473-480.
- [4] K. Huh, J. Kim and J. Hong, Handling and driving characteristics for six-wheeled vehicle, *Proceedings of the Institution of Mechanical Engineers, Part D, Journal of Automobile Engineering*, 214 (2) (2000) 159-170.
- [5] A. Jackson and D. Crolla, Improving performance of a 6x6 off-road vehicle through individual wheel control, *SAE2002*, 2002-01-0968.
- [6] B. C. Chen, C. C. Yu and W. F. Hsu, Optimal steering control for six-wheeled vehicle, *Proceeding of International Symposium on Advanced Vehicle Control* (2006) 605-610.
- [7] S. J. An, H. Y. Lee, W. K. Cho, G. Jung, K. Yi and K. Lee, Development of steering algorithm for 6WS military vehicle and verification by experiment using a scale-down vehicle, *Proc. Int. Symp. Advanced Vehicle Control* (2006) 245-250.
- [8] S. J. An et al., Desired yaw rate and steering control method during cornering for a six-wheeled vehicle, *IJAT*, 9 (2) (2008) 173-181.

- [9] O. Mokhiamar and M. Abe, Simultaneous optimal distribution of lateral and longitudinal tire forces for the model following control, *Journal of Dynamic Systems, Measurement of Control*, 126 (2004) 753-763.
- [10] R. Kenneth and Buckholtz, Reference input wheel slip tracking using sliding mode control, *SAE World Congress* (2002) 2002-01-0301.
- [11] W. Kim, J. Kang, K. Yi and J. Lee, Development of driving control system based on optimal distribution for a 6WD/6WS vehicle, *SAE Int. J. of Passeng. Cars – Mech. Syst.* (3) 145-157, August 2010.
- [12] J. Kang and K. Yi, Development and validation of a finite preview optimal control based human driver steering model, *KSAE spring conference* (2007) 855-860.



Wongun Kim received the B.S. and M.S. in Mechanical Engineering and Mechanical Design Engineering from Hanyang University, Korea, in 2005 and 2007, respectively. Since 2008, he has been a Ph.D. candidate in the program in automotive engineering at Seoul National University, Korea. His

research interest is autonomous military combat vehicles.



Jongseok Lee received the B.S. and M.S. in Mechanical Engineering from Pukyong National University, Korea, in 1997 and 1999, respectively. He is working at SAMSUNG TEKWIN in Korea. His research interests are drive control systems and active safety systems of a ground vehicle.



Kyongsu Yi received the B.S. and M.S. in Mechanical Engineering from Seoul National University, Korea, in 1985 and 1987, respectively, and the Ph.D. from the University of California, Berkeley, in 1992. Dr. Yi is a Professor of the School of Mechanical and Aerospace Engineering at Seoul National University,

Korea. He currently serves as a member of the editorial boards of the KSME, IJAT and ICROS journals. Dr. Yi's research interests are control systems, driver assistant systems, and active safety systems of a ground vehicle.